ABC-Model for Interpretation of Internal Quantum Efficiency and Its Droop in III-Nitride LEDs: A Review

SERGEY KARPOV*

STR Group – Soft-Impact, Ltd., P.O.Box 83, 27 Engels ave., St.Petersburg, 194156 Russia
(E-mail: sergey.karpov@str-soft.com)

Abstract. The paper reviews applications of ABC-model to interpret internal quantum efficiency and its droop in III-nitride light-emitting diodes. Advantages of the model, its intrinsic limitations, and tentative mechanisms responsible for deviation of the model predictions from available observations are discussed. New experimental information on recombination processes in the LED active regions coming in terms of the ABC-model is considered along with still open questions and tasks for further experimental and theoretical researches.

Key words: III-nitrides, light-emitting diodes, recombination, efficiency droop, ABC-model

1 Introduction

One of the challenges for development of state-of-the-art light-emitting diodes (LEDs) is the increase of their output optical power at the same device area. This requires the LEDs to operate at elevated current densities, normally resulting in the efficiency droop, i.e. reduction of the light emission efficiency with the forward current driving the diode. A natural reason for the droop is the device self-heating – see, e.g. Chen *et al.* (2008), though contribution of non-thermal mechanisms may be considerable in some cases, especially in the LEDs made of III-nitride semiconductors (Mukai *et al.* 1999; Krames *et al.* 2000). While the conventional way for decreasing the thermal droop implies reduction of the LED thermal resistance, suppression of the non-thermal droop needs a comprehensive understanding of the mechanisms underlying this phenomenon. In particular, the nature of the non-thermal droop in InGaN-based LEDs was debated for a long time, choosing eventually between the carrier overflow/spillover/leakage from the active region (Rozhansky and Zakheim 2006; Kim *et al.* 2007) and non-radiative Auger recombination (Shen *et al.* 2007; Bulashevich and Karpov 2008; Laubsch *et al.* 2009) – see also (Piprek 2010; Verzellesi *et al.* 2013) for more detailed review of the problem.

In the lack of experimental techniques capable of unambiguous identifying the non-thermal droop mechanisms, arguments based on modeling and simulations become of primary importance. Here the simplest and, perhaps, the most popular approach is that based on the ABC-model considering three principal channels of the electron and hole recombination in the LED active region: non-radiative Shockley-Read-Hall recombination, radiative recombination, and non-radiative Auger recombination. In particular, the ABC-model has been invoked to explain the non-thermal droop in InGaN-based LED structures in terms of Auger recombination, being in good agreement with available observations of (Shen *et al.* 2007; Laubsch *et al.* 2009). Since that time, the ABC-model is extensively applied to variety of data to find *pro* and *contra* for the idea of the dominant role of Auger recombination in the non-thermal droop of III-nitride LED efficiency and to examine ways for improvement of LED structure designs. Moreover, a considerable portion of experimental information on the recombination processes in LED structures comes today largely in terms of the ABC-model. One more reason for the wide popularity of the ABC-model is its capability of excellent fitting the efficiency behavior of high-quality blue LEDs under variation of their

operating current in a wide, ~5-7 orders of magnitude, range – see, e.g. (Titkov *et al.* 2014) and Sec.2.1 for more examples.

On the other hand, the ABC-model is severely criticized for oversimplified treatment of the considered physical processes and for some disagreements with a number of observations largely made in the green spectral range – see, e.g. (Dai *et al.* 2011). Including additional terms depending on the non-equilibrium carrier concentration to the power higher than third has been suggested in a number of papers to improve the model predictability (Eliseev *et al.* 1999; Dai *et al*. 2010). This provides a better fitting of some experimental data but does not generally clarify the physics behind.

This paper is aimed at reviewing strong and weak points of the ABC-model, analyzing physical mechanisms responsible for deviations of available observations from the model predictions, and discussing the issues for which the model may provide valuable information, as well as the problems still waiting for more detailed experimental and theoretical investigations.

2 ABC model: advantages and limitations

2.1 Practical formulation and opportunities for the efficiency analysis

The simplest ABC-model is derived under rather strict assumptions. First, the electron leakage from the active region is neglected, providing a balance between the current flowing through the LED structure and integral recombination rate. Second, the non-equilibrium concentrations of electrons n and holes p in the LED active region are assumed to be equal to each other. Third, the constant A corresponding to the Shockley-Read-Hall (SRH) non-radiative recombination, the constant B corresponding to the bimolecular radiative recombination, and the constant C associated with the non-radiative Auger recombination are assumed to be nearly independent of the carrier concentration. In this case, the operating current I, output optical power P_{out}, and external quantum efficiency (EQE) η_e of an LED can be expressed through the carrier concentration n as follows:

$$I = qV_R(An + Bn^2 + Cn^3) \quad , \quad P_{out} = E_{ph}\eta_{ext}V_R Bn^2$$
$$\eta_e = \frac{qP}{E_{ph}I} = \eta_{ext}\eta_i \quad , \quad \eta_i = \frac{Bn}{A + Bn + Cn^2} \tag{1}$$

Here q is the electron charge, E_{ph} is the photon energy averaged over the LED emission spectrum, V_R is the recombination volume, i.e. the volume of the active region with intensive carrier recombination, η_i is the internal quantum efficiency (IQE) of light emission, and η_{ext} is the light extraction efficiency (LEE) of the LED chip also assumed to be independent of the carrier concentration/operating current.

As the non-equilibrium carrier concentration can hardly be measured in practice, it should be excluded from Eq.(1) by expressing via observable variables. It has been found in earlier applications of the ABC-model, that the IQE dependence on operating current is controlled by only two parameters: the peak IQE value $\eta_i^{\max}$ and the current I_m corresponding to the IQE peak (Ryu et al. 2009). The latter parameter could be found directly from EQE measured as a function of current, while the former one required fitting to the whole $\eta_e(I)$ curve. To derive the full dependence $\eta_i(I)$, a cubic equation has been suggested in (Ryu et al. 2009), being not so suitable for operative estimations.

Advantages of the ABC-model become clear, if η_e is plotted *versus* output optical power P_{out}, then the power P_m corresponding to the EQE maximum η_e^{max} is found from the plot, and, finally, η_e is plotted as a function of the normalized optical power (NOP) $P = P_{out}/P_m$. In this case, the ABC-model provides analytical expressions for EQE, IQE, and the maximum IQE value (Dai *et al*. 2010):

$$\eta_e(P) = \eta_{ext}\eta_i \quad , \quad \eta_i = \frac{Q}{Q + P^{1/2} + P^{-1/2}} \quad , \quad \eta_i^{max} = \frac{Q}{Q+2} \quad , \qquad (2)$$

where the quality factor $Q = B/(AC)^{1/2}$ is a dimensionless invariant of the ABC-model. Being directly related to the maximum IQE value, the Q-factor may serve as the figure of merit for comparing LED structures of different designs or those operating in different spectral ranges (Bulashevich *et al.* 2012).

Plotting the η_e^{max}/η_e ratio *versus* $P^{1/2} + P^{-1/2}$, approximating the plot by a linear function, and finding the cross point of the line with the vertical axis, one can determine the maximum IQE value, Q-factor, and LEE as the $\eta_e^{max}/\eta_i^{max}$ ratio – see Fig.1a and (Titkov *et al.* 2014). Then η_e as a function of P can be calculated by using Eq.(2). Figure 1b demonstrates application of the above procedure to the data reported in (Schiavon *et al.* 2012), providing good fitting of the EQE behavior in a wide range of NOP or, the same, operating current variation. One can see the data deviations from the ABC-model predictions to occur either at low or at high values of NOP, which manifests itself in Fig.1a by a slight non-linearity of the experimental η_e^{max}/η_e dependence observed at high $P^{1/2} + P^{-1/2}$.

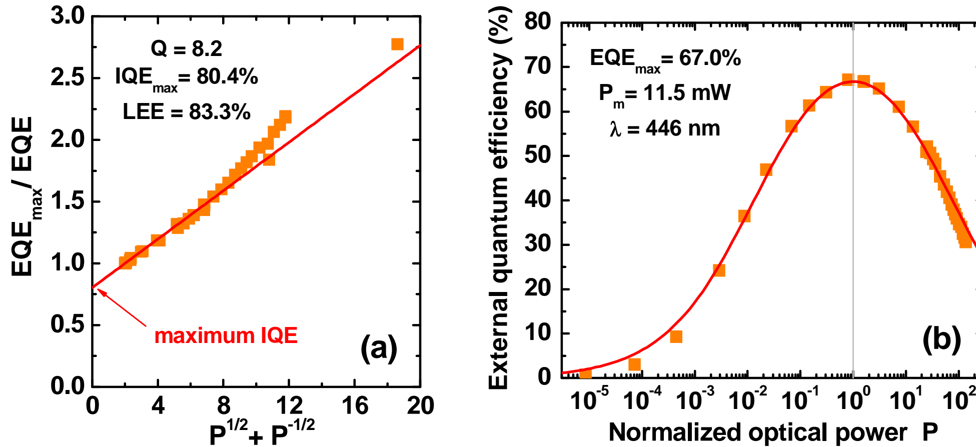

Fig. 1 η_e^{max}/η_e ratio as a function of $P^{1/2} + P^{-1/2}$ (a) and measured room-temperature EQE of a blue LED as a function of NOP (b). Squares indicate the data obtained at Osram OS (Schiavon *et al.* 2012), lines are fittings of the data by the ABC-model.

According to Eq.(1), EQE η_e being plotted *versus* NOP in a logarithmic scale, should provide a curve with the even symmetry relatively to the line corresponding to $P = 1$ – see, e.g., (Dai *et al.* 2001) and Fig.1b. In practice, the symmetry is frequently broken, especially in the case of green LEDs, where the low-current wing of the $\eta_e(I)$ dependence is normally more extended than the high-current one. The mechanisms tentatively responsible for low-current and high-current deviations from the ABC-model predictions and their correlations with available observations are considered below in more detail.

2.2 Low-current emission efficiency

Two important mechanisms may additionally control the LED efficiency at low operating currents/NOPs. One is the electron/hole localization by composition fluctuations in the InGaN quantum wells (QWs) (Chichibu *et al*, 2006; Karpov 2010). The fluctuations form indium-rich inclusions in the QWs capable of capturing the non-equilibrium carriers, thus preventing them from lateral movement in the QW followed by non-radiative recombination at threading dislocations. As a result, the rate of the SRH recombination becomes dependent on the localization energy related to fluctuations, as well as on temperature and quasi-Fermi level positions relatively to the conduction and valence band edges – see (Karpov 2010) for detail of theoretical model.

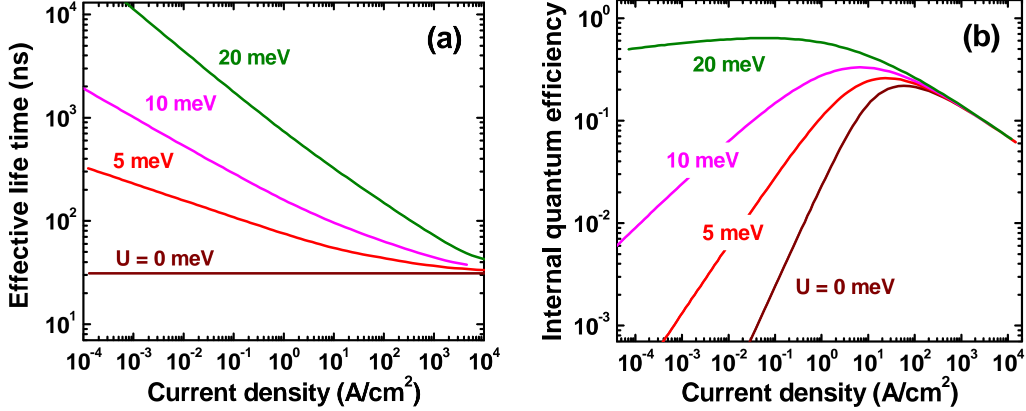

Fig. 2 Room-temperature effective carrier life time A^{-1} (a) and IQE (b) as a function of the current density calculated by ABC-model accounting for the effect of composition fluctuations in 2.5 nm green InGaN SQW on non-radiative carrier recombination at threading dislocations. The curves correspond to various localization energies U . The recombination constants $B = 1\times10^{-12}$ cm^3/s and $C = 1\times10^{-31}$ cm^6/s were used in the calculations.

Figure 2a shows the effective carrier life time equal to A^{-1} as a function of current density j calculated by ABC-model with account of the composition fluctuation effect on the non-radiative carrier recombination at threading dislocations. For simplicity, the same localization energy U was assumed in the calculations for both electrons and holes. At $U = 0$, the effective life time is independent of the current density, corresponding to the value predicted by the model of dislocation-mediated carrier recombination (Karpov and Makarov 2002). At $U > 0$ the life time grows substantially at low currents (Fig.2a). This leads to a slope modification of the low-current wing in the $\eta_i(j)$ dependence, whereas the high-current wing remains unchanged (Fig.2b).

Another mechanism that may affect the low-current IQE is breaking of the QW electric neutrality originated from different concentrations of electrons and holes injected into the well. This results in IQE which does not vanish at low currents but tends to a constant value $(1 + N_* / N + N / N_* Q_*^2)^{-1}$ where the concentration $N_* = (B\tau_p)^{-1}$ and the dimensionless parameter $Q_* = B(\tau_p / C_n)^{1/2}$, if the electron concentration exceeds that of holes by the value N; if the hole concentration exceeds that of electrons by N, then $N_* = (B\tau_n)^{-1}$ and $Q_* = B(\tau_n / C_p)^{1/2}$ (Galler *et al.* 2013). Here, τ_n and τ_p are the partial non-radiative life times of electrons and holes ($\tau_n + \tau_p = A^{-1}$), whereas C_n and C_p are the Auger recombination constants corresponding to the microscopic processes

involving either two electrons and a hole (*nnp*-process) or two holes and an electron (*npp*-process), respectively ($C_n + C_p = C$).

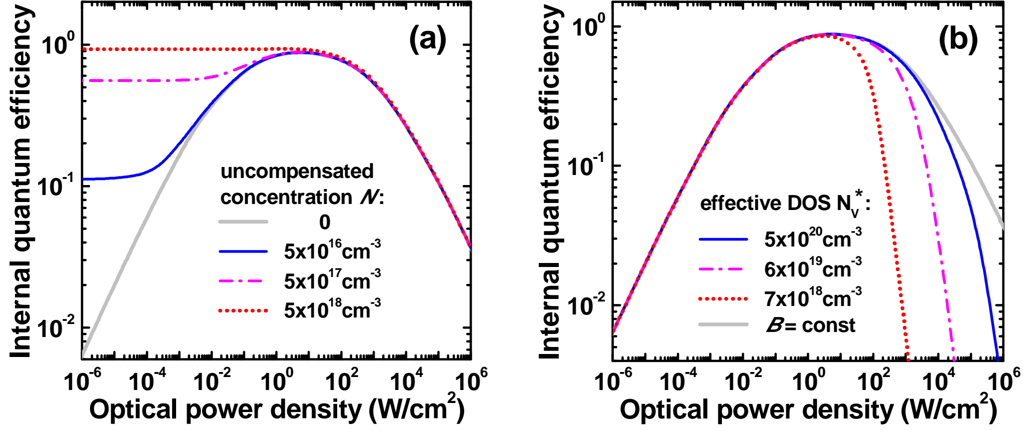

Fig. 3 IQE *versus* optical power density calculated for the case of (a) deviation from the electric neutrality in the QW and (b) degeneration of holes. Calculations were made for 3 nm SQW emitting at 450 nm and recombination constants $A = 10^6$ s^{-1}, $B = 5\times10^{-12}$ cm^3/s, and $C = 1\times10^{-31}$ cm^6/s.

Using the ABC-model modification suggested in (Galler *et al.* 2013), one can obtain the IQE as a function of emitted optical power density (Fig.3a), where the breaking of the QW electric neutrality affects primarily the low-current wing of the $\eta_i(P_{out})$ dependence. Such a behavior is not, however, observed in practice. Nevertheless, assuming the excess concentration N to be a function monotonically rising with the current density, one can obtain the low-current wing in the $\eta_i(I)$ dependence similar to the observed ones. A tendency to the current-dependent violation of the electric neutrality in InGaN QWs has been predicted theoretically for both polar and non-polar LED structures (Kisin *et al.* 2012; Kisin *et al.* 2013).

At the moment, one cannot conclude reliably what of the above two mechanisms is dominant at low-current LED operation. Therefore, this remains an open question for further studies.

2.3 High-current emission efficiency

A number of mechanisms may be responsible for high-current deviations of the efficiency behavior from that predicted by the ABC-model. The most straightforward one is the LED self-heating. To avoid its contribution to experimental results, the EQE measurements should be carried out under pulsed injection, at least at high currents, with the use of a good heat sink, which is not always takes place. One more mechanism is related to chip designs utilizing metallic electrodes formed to the emitting surfaces of LED dice. In this case, current crowding enhanced at high operating currents leads to localization of the photon-emission region under the electrodes, thus increasing the optical losses caused by incomplete light reflection from the metal. As a result, the light extraction efficiency from the LED die becomes current-dependent, increasing the EQE droop at high currents (Bogdanov *et al.* 2010). The use of the state-of-the-art flip-chip designs with one-side electrode access to both n- and p-contact layers (Shchekin *et al.* 2006; Laubsch *et al.* 2010) enables considerable reduction of the above shading effect. Even in this case, however, the current crowding still contributes to the LED efficiency droop at high currents because of violation of the proportionality between the averaged current density $\overline{j} = I^{-1}\int_S j^2(\mathbf{r})\,d^2\mathbf{r}$ and the operating

current I, which is normally assumed in the data analysis (the integration in the above formula is made over the whole area S of the active region).

Another high-current mechanism frequently discussed in literature is the electron leakage into p-side of an LED structure (Rozhansky and D. A. Zakheim 2006; Kim *et al.* 2007; Piprek 2010). Its impact on the emission efficiency largely depends on the LED structure design and can be minimized by careful bandgap engineering. According to (Piprek 2010), manifestations of this mechanisms can hardly be distinguished from those caused by Auger recombination. In contrary, our simulations usually demonstrate a noticeable changes in the slope of the $\eta_i(I)$ dependences at high currents, correlating with the onsets of electron leakage. The difference in the above conclusions may be attributed, at least partly, to the difference in the material properties chosen for simulations (Piprek and Li 2013).

Band-filling effect is also commonly considered as a reason of the high-current deviations from the predictions of ABC-model. Assuming the electron effective mass to be much lighter than the hole one, one can derive a semi-empirical dependence for the radiative recombination constant of a bulk semiconductor: $B(p)=[\tau_R(N_V^{3D}+p)]^{-1}$, where p is the non-equilibrium hole concentration, N_V^{3D} is the effective 3D density of states in the valence band, $\tau_R = m_0^2c^3\hbar^2/4n_rq^2E_G\overline{M_{cv}^2}$ is the specific radiation time, m_0 is the electron mass, c is the light velocity, $\hbar$ is the Plank's constant, n_r and E_G are the refractive index and bandgap of the semiconductor, respectively, and $\overline{M_{cv}^2}$ is the square of the matrix element of the optical transition averaged over the photon polarization. Developing the above expression for B as series in p/N_V^{3D}, one can formally obtain the negative terms of the order higher than third in the expression for the total recombination rate as a function of carrier concentration.

However, the same assumptions applied to a narrow QW, i.e. that having only the ground states of electrons and holes, provide a different expression for the radiative recombination constant: $B(p)=[1-\exp(-p/N_V^*)]/(p\tau_R)$, where $N_V^* \cong N_V^{2D}/d$, N_V^{2D} is the effective 2D valence-band density of states in the QW and d is the QW width. This expression predicts an exponentially fast reduction of the B-constant with the hole concentration, in contrast to the power-like dependence typical for bulk materials. This means, in particular, that the B-constant reduction become substantial only if holes are degenerate. The degeneration occurs when the hole concentration become higher than N_V^*, which is ~6-7×10^{19} cm^{-3} at 300 K in typical InGaN QWs. To achieve such a high hole concentrations, the current densities between 100 and 1000 A/cm^2 are required. At low temperatures, however, N_V^* decreases considerably, and the hole degeneration should start at remarkably lower current densities, resulting in a stronger IQE droop at high currents (Fig.3b).

Experiments provide contradictory information on the observed EQE behavior as a function of temperature. The data reported in (Fudjiwara *et al.* 2009; Shin *et al.* 2012) likely demonstrate an evident shift of the current corresponding to the hole degeneration to lower values under the temperature decrease. In contrast, the careful temperature measurements made with commercial blue LEDs do not reproduce this effect (Laubsch *et al.* 2009; Titkov *et al.* 2014). Therefore, it is still unclear, if the band-filling effect is valuable at high currents in state-of-the-art LEDs or not.

3 Recombination constants

Being estimated from experiments, two invariant of the ABC-model, Q-factor and $P_m = E_{ph}\eta_{ext}V_R(BA/C)$, cannot determine unambiguously three recombination constants A, B, and C. This, however, becomes possibly by invoking additional data like measurements of differential carrier life time (DLT) *versus* operating current (Eliseev *et al.* 1999; David and Grundmann 2010a; Schiavon *et al.* 2012). According to the ABC-model, DLT measured as a function of NOP enables fitting by the theoretical dependence $\tau_D = A^{-1}/(1+2QP^{1/2}+3P)$ with the only free parameter A. As soon, as the recombination constant A is determined from the fitting, the other constants can be found using the relationships:

$$C = A^3Q^2(V_R/R_m)^2\ ,\ \ B = A^2Q^2(V_R/R_m)\ \ ;\ \ R_m = P_{out}/E_{ph}\eta_{ext} \tag{3}$$

Detailed measurements of the recombination constants carried out in a wide spectral range of 440-530 nm have been reported in (Schiavon *et al.* 2012) for SQW LED structures grown on sapphire substrates. The use of the SQW active region excluded uncertainty in the choice of the recombination volume normally arising in the case of MQW LEDs. The results of the measurements are given in Fig.4. One can see from the figure that the A constant is practically invariable between 440 and 510-515 nm but it exhibits a dramatic rise at longer emission wavelengths (the point corresponding to the wavelength of 470 nm seems here to be an outlier). The rise in the A constant, which is not accompanied by noticeable changes in the behavior of B and C constants, can be attributed to intensive defect generation in the high-indium content QWs. The Auger recombination constant C is found to be weakly dependent on the emission wavelength (Fig.4a), whereas its value and spectral dependence agree reasonably with the recent theoretical estimates reported in (Kioupakis *et al.* 2011).

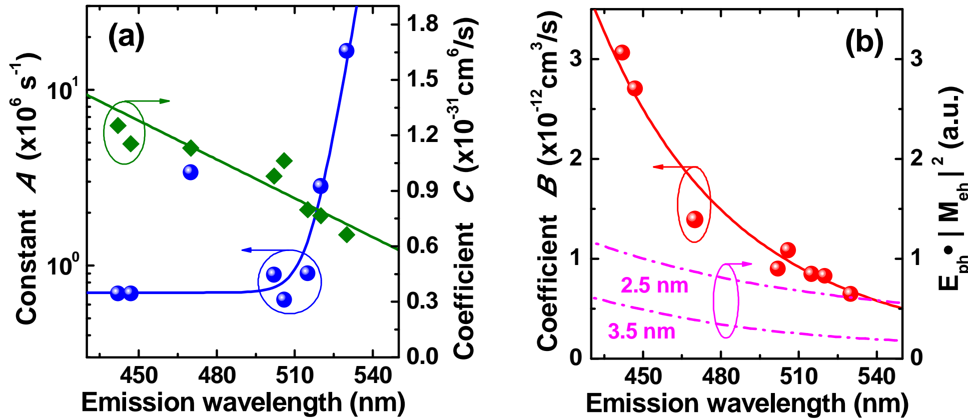

Fig. 4 Recombination constant A and C (a), recombination constant B , and computed product of the emitted photon energy E_{ph} and the square of the overlap integral $|M_{eh}|^2$ between electron and hole wave functions (dash-dotted lines) (b) in SQW LED structures as a function of the emission wavelength. Symbols are experimental points from (Schiavon *et al.* 2012), solid lines are drawn for eyes.

The experimental radiative recombination constant B decays almost six times with the emission wavelength varied from 440 to 530 nm (Fig.4b). Even stronger decrease of the B constant with the wavelength was earlier reported in (David and Grundmann 2010b). Such a rapid decay does not correspond to the theoretical estimates made for SQW LED structures using the conventional **k·p** approach. Indeed, the calculated overlap integral of the ground-state electron and hole wave functions multiplied by the photon energy exhibits only twofold decay in the same spectral range, irrespec-

tively of the QW width (see Fig.4b, right axis). The origin of the rapid decay of the experimental *B* constant is not clear at the moment and requires further investigations.

One more unexpected behavior of the recombination constants has been revealed by Hader *et al.* (2011). Calculating theoretically the constant *B* and using the EQE data of Fudjiwara *et al.* (2009) to evaluate other recombination coefficients, Hader *et al.* (2011) concluded that the Auger coefficient *C* should decay with temperature. A similar finding was reported for InGaN quantum-dot (QD) laser diodes emitting at 630 nm (Frost *et al.* 2014). Being in some conflict with the existing theories (Kioupakis *et al.* 2011; Bertazzi *et al.* 2012; Vaxenburg *et al.* 2013), the above phenomenon cannot be, nevertheless, considered as unphysical. Indeed, the Auger coefficient decaying with temperature was observed in heavily doped p-SiC by Galeckas *et al.* (2013) and predicted theoretically for specific non-threshold Auger processes in low-dimensional structures, QWs and QDs, where the momentum conservation is violated in some directions (Dyakonov and Kachorovskii 1994; Polkovnikov and Zegrya 1998).

Despite the recent progress in the theory of Auger recombination in III-nitride heterostructures (Kioupakis *et al.* 2011; Bertazzi *et al.* 2012; Vaxenburg *et al.* 2013), there still remains a number of open questions. One of them is identification of the dominant microscopic Auger process. The *nnp*-process involving two electrons and a hole has been directly observed by monitoring the hot-electron emission from a specially prepared LED structure under current injection (Iveland *et al.* 2013). More recent experiments have pointed out that the *npp*-process involving two holes and an electron may also be important (Binder *et al.* 2013), though the former process is, nevertheless, dominating, at least, in blue LED structures (Galler *et al*. 2013). Being very important for practice, this conclusion requires additional experimental confirmation and quantitative theoretical justifications.

4 Outlook for future studies

Up to date, the ABC-model is serving as a bridge between the experimental and theoretical studies of recombination processes in III-nitride LED structures, providing new valuable information and putting forward new tasks for further research. Among these tasks the most urgent seem to be: (i) measuring and modeling the basic temperature and wavelength dependences of the recombination constants in SQW and MQW LED structures, (ii) understanding the crystal orientation effect on the recombination constants, (iii) understanding the nature of the 'green gap' in the LED efficiency in terms of interplay between various recombination channels, and (iv) identification of dominant microscopic mechanisms of Auger recombination in typical LED structures.

A separate task is linking/comparing the ABC-model with advanced simulation approaches, which has, in particular, to explain why the ABC-model is capable to fit well EQE of high-quality blue LEDs in so wide range of the operating currents, in spite of the evident limitations and simplifications of the model. Understanding the role of carrier localization for various recombination channels in InGaN-based active regions under low-current and high-current conditions and its dependence on the InGaN composition would also be rather important.

The above review did not consider possible variation of the recombination volume V_R with current and its impact on the efficiency of LED structures. Strictly speaking, this problem is beyond the scope of the simple ABC-model and requires detailed analysis of non-equilibrium electron and hole transport across the structures. Being largely avoided in SQW active regions, the above problem may become important in the case

of MQW structures (David *et al.* 2008; Galler *et al.* 2011). This aspect requires detailed examination, especially in view of advantageous exploiting the MQW structures with extremely narrow barriers providing strong coupling between the QWs (Zakheim *et al*. 2011).

Acknowledgments: This work was supported by European Union FW7 program, NEWLED project, grant number 318388. Many thanks to Bastian Galler and Michael Binder from Osram Opto Semiconductors for providing detailed data and valuable discussions.

References

Bertazzi, F., X. Zhou, M. Goano, G. Ghione and E. Bellotti. *Appl. Phys. Lett.* **103** 081106, 2012.
Binder, M., A. Nirschl, R. Zeisel, T. Hager, H.-J. Lugauer, M. Sabathil, D. Bougeard, J. Wagner and B. Galler. *Appl. Phys. Lett.* **103** 071108, 2013.
Bogdanov, M. V., K. A. Bulashevich, O. V. Khokhlev, I. Yu. Evstratov, M. S. Ramm and S. Yu. Karpov. *Phys. Stat. Solidi C* **7** 2124, 2010.
Bulashevich, K. A. and S. Yu. Karpov. *Phys. Stat. Solidi C* **5** 2066, 2008.
Bulashevich, K. A., O. V. Khokhlev, I. Yu. Evstratov and S. Yu. Karpov. *Proc. SPIE* **8278** 827819, 2012.
Chen, T.P., C.L. Yao, C.Y. Wu, J.H. Yeh, C.W. Wang and M.H. Hsieh. *Proc. SPIE* **6910** 691005-1, 2008.
Chichibu, S. F., A. Uedono, T. Onuma, B. A. Haskell, A. Chakraborthy, T. Koyama, P. T. Fini, S. Keller, S. P. DenBaars, J. S. Speck, U. K. Mishra, S. Nakamura, S. Yamaguchi, S. Kamiyama, H. Amano, I. Akasaki, J. Han and T. Sota, Nature materials **5** 810, 2006.
Dai, Q., Q. Shan, J. Wang, S. Chhajed, J. Cho, E. F. Schubert, M. H. Crawford, D. D. Koleske, M.-H. Kim and Y. Park. *Appl. Phys. Lett.* **97** 133507, 2010.
Dai, Q., Q. Shan, J. Cho, E. F. Schubert, M. H. Crawford, D. D. Koleske, M.-H. Kim and Y. Park. *Appl. Phys. Lett.* **98** 033506, 2011.
David, A., M. J. Grundmann, J. F. Kaeding, N. F. Gardner, T. G. Mihopoulos and M. R. Krames. *Appl. Phys. Lett.* **92** 053502, 2008.
David A. and M. J. Grundmann. *Appl. Phys. Lett.* **96** 103504, 2010a.
David A. and M. J. Grundmann. *Appl. Phys. Lett.* **97** 033501, 2010b.
Dyakonov M. I. and V. Yu. Kachorovskii. *Phys. Rev. B.* **49** 17130, 1994.
Eliseev, P. G., M. Osin'ski, H. Li and I. V. Akimova. *Appl. Phys. Lett.* **75** 3838, 1999.
Frost, T., A. Banerjee, S. Jahangir and P. Bhattacharya. *App. Phys. Lett.* **104** 081121, 2014.
Fudjiwara, K., H. Jimi and K. Kaneda. *Phys. Stat. Solidi C* **6** S814, 2009.
Galeckas, A., J. Linnros, V. Grivickas, U. Lindefelt and C. Hallin. *Appl. Phys. Lett.* **102** 031120, 2013.
Galler, B., A. Laubsch, A. Wojcik, H. Lugauer, A. Gomez-Iglesias, M. Sabathil and B. Hahn. *Phys. Stat. Solidi C* **8** 2372, 2011.
Galler, B., H.-J. Lugauer, M. Binder, R. Hollweck, Y. Folwill, A. Nirschl, A. Gomez-Iglesias, B. Hahn, J. Wagner and M. Sabathil. *Appl. Phys. Express* **6** 112101, 2013.
Hader, J., J. V. Moloney and S. W. Koch. *Appl. Phys. Lett.* **99** 181127, 2011.
Iveland, J., L. Martinalli, J. Peretti, J. S. Speck and C. Weisbuch. *Phys. Rev. Lett.* **110** 177406, 2013.
Karpov, S. Yu. and Yu. N. Makarov. *Appl. Phys. Lett.* **81** 4721, 2002.
Karpov, S. Yu. Phys. *Stat. Solidi RRL* **4** 320, 2010.
Kim, M.-H., M. F. Schubert, Q. Dai, J. K. Kim, E. F. Schubert, J. Piprek and Y. Park. *Appl. Phys. Lett.* **91** 183507, 2007.
Kioupakis, E., P. Rinke, K. T. Delaney and C. G. Van de Walle. *Appl. Phys. Lett.* **98** 161107, 2011.
Kisin, M. V., C.-L. Chuang and H. S. El-Ghoroury. *Semicond. Sci. Technol.* **27** 024012, 2012.
Kisin, M. V., C.-L. Chuang and H. S. El-Ghoroury. *J. Appl. Phys.* **111** 103113, 2013.
Krames, M. R. , G. Christenson, D. Coffins, L. W. Cook, M. G. Craford, A. Edwards, R. M., Fletcher, N. Gardner, W. Goetz, W. Imler, E. Johnson, R. S. Kern, R. Khare, F. A. Kish, C., Lowery, M. J. Ludowise, R. Mann, M. Maranowski, S. Maranowski, P. S. Martin, J. O'Shea, S., Rudaz, D. Steigerwald, J. Thompson, J. J. Wierer and J. Yu. *Proc. SPIE* **3938** 2, 2000.
Laubsch, A., M. Sabathil, W. Bergbauer, M. Strassburg, H. Lugauer, M. Peter, S. Lutgen, N. Linder, K. Streubel, J. Hader, J. V. Moloney, B. Pasenow and S. W. Koch. *Phys. Status Solidi C* **6** S913, 2009.
Laubsch, A., M. Sabathil, J. Baur, M. Peter and B. Hahn. *IEEE TED* **57** 79, 2010.
Mukai, T., M. Yamada and S. Nakamura. *Jpn. J. Appl. Phys.* **38** 3976, 1999.
Piprek, J. *Phys. Stat. Solidi A* **207** 2217, 2010.
Piprek, J. and S. Li. *Appl. Phys. Lett.* **102** 131103, 2013.

Polkovnikov, A. S. and G. G. Zegrya. *Phys. Rev. B* **58** 4039, 1998.
Rozhansky, I. V. and D. A. Zakheim. *Semiconductors* **40** 839, 2006.
Ryu, H.-Y. H.-S. Kim and J.-I. Shim. *Appl. Phys. Lett.* **95** 081114, 2009.
Shchekin, O. B., J. E. Epler, T. A. Trottier, T. Margalith, D. A. Steigerwald, M. O. Holcomb, P. S. Martin and M. R. Krames. *Appl. Phys. Lett.* **89** 071109, 2006.
Schiavon, D., M. Binder, M. Peter, B. Galler, P. Drechsel and F. Scholz. *Phys. Stat. Solidi B* **250** 283, 2012.
Shen, Y. C., G. O. Müller, S. Watanabe, N. F. Gardner, A. Munkholm and M. R. Krames. *Appl. Phys. Lett.* **91** 141101, 2007.
Shin, D.-S., D.-P. Han, Ji.-Y. Oh and J.-I. Shim. *Appl. Phys. Lett.* **100** 153506, 2012.
Titkov, I. E., S. Yu. Karpov, A. Yadav, V. L. Zerova, M. Zulonas, B. Galler, M. Strassburg, I. Pietzon-ka, H.-J. Lugauer and E. U. Rafailov. submitted to *IEEE JQE*
Vaxenburg, R., E. Lifshitz and Al. L. Efros. *Appl. Phys. Lett.* **102** 031120, 2013.
Verzellesi, G., D. Saguatti, M. Meneghini, F. Bertazzi, M Goano, G. Meneghesso and E. Zanoni. *J. Appl. Phys.* **114** 071101, 2013.
Zakheim, D. A., A. S. Pavluchenko and D. A. Bauman. Phys. *Status Solidi C* **8** 2340, 2011.